

Are extrasolar Einstein's spinning tops habitable?

Lorenzo Iorio¹

Ministero dell'Istruzione, dell'Università e della Ricerca (M.I.U.R.)

Viale Unità di Italia 68, I-70125, Bari (BA), Italy

`lorenzo.iorio@libero.it`

Received _____; accepted _____

Abstract

Recently, the possibility that putative massive natural satellites (exomoons) of extrasolar Jupiter-like giant planets orbiting main sequence stars may be habitable has gained increasing attention. Typically, such an exomoon is expected to orbit its parent planet in the equatorial plane of the latter, with its spin \mathbf{S} aligned with its orbital angular momentum \mathbf{L} which, in turn, is parallel to the planetary spin \mathbf{J} . If, in particular, the common tilt of such angular momenta to the satellite-planet ecliptic plane, assumed fixed, has certain values, the overall irradiation experienced by the exomoon from the star may allow it to sustain life as we know it, at least for certain orbital configurations. A telluric body orbiting different gaseous giant primaries at $5 - 10$ planetary radii R whose spin is initially tilted to the ecliptic by the same angle $\varepsilon_0 = 23^\circ.44$ as Earth is considered. Here, I show that, by allowing more or less large departures from the merely ideal condition of exact alignment of \mathbf{S} , \mathbf{L} , \mathbf{J} , the general relativistic de Sitter and Lense-Thirring precessions of the satellite's spin due to the post-Newtonian (pN) field of the host planet may have a non-negligible impact on the exomoon's habitability through induced long-term variations $\Delta\varepsilon(t)$ of the obliquity ε of the satellite's spin \mathbf{S} to the ecliptic plane which may be as large as tens of degrees over $\simeq 0.1 - 1$ millions of years.

Subject headings: Planets and satellites: general – Astrobiology – Gravitation – Celestial mechanics – Methods: analytical – Methods: numerical

1. Introduction

In investigating the possibility that alien worlds, in particular extrasolar planets¹ (Seager 2011; Lissauer 2012; Deeg & Belmonte 2018; Perryman 2018) and related environments, may host and sustain known (and unknown) forms of life and, possibly, civilizations (Kaltenegger 2017; Schulze-Makuch & Bains 2018; Schwieterman et al. 2018; Irwin & Schulze-Makuch 2020), it is of crucial importance to assess, among other things, the physical conditions posing more or less tight constraints on such an opportunity. In this framework, I will look at a novel scenario which has recently gained growing attention by demonstrating that, under certain circumstances, the Einstein’s General Theory of Relativity (GTR; Debono & Smoot 2016; Misner, Thorne & Wheeler 2017) may have a direct, macroscopic impact on life and its long-term sustainability in a likely soon testable astronomical context.

Despite they have not yet been discovered, possible natural satellites of planetary size, dubbed as exomoons (Barnes & O’Brien 2002; Domingos, Winter & Yokoyama 2006; Heller et al. 2014; Schneider, Lainey & Cabrera 2015), orbiting Jupiter-like gaseous giants irradiated by main sequence stars have recently attracted increasing interest because, among other things, they may be habitable (Williams, Kasting & Wade 1997; Kaltenegger 2010; Heller, R. 2012; Forgan & Kipping 2013; Heller & Barnes 2013; Hinkel & Kane 2013; Heller et al. 2014; Dobos, Heller & Turner 2017; Zollinger, Armstrong & Heller 2017; Hill et al. 2018; Forgan, D. 2019; Martínez-Rodríguez et al. 2019; Lingam & Loeb 2020; Tjoa, Mueller & van der Tak 2020). Their mass m should be $0.25 m_{\oplus} \lesssim m \lesssim 2 m_{\oplus}$ to sustain life over a billion-year timescale (Heller & Barnes 2013). According to Sasaki, Stewart & Ida (2010), their actual formation around extrasolar giant planets is possible. Still unconfirmed exomoons candidates exist (Fox & Wiegert 2021; Teachey & Kipping 2018). The project Hunt for Exomoons with Kepler (HEK) was the most important effort aimed to detect exomoons to date (Kipping et al. 2012, 2013b,a; Teachey, Kipping & Schmitt 2018). Searches for exomoons started in 2009 (Kipping 2009a,b; Kipping, Fossey & Campanella 2009), after theoretical investigations about such a possibility (Sartoretti & Schneider 1999; Cabrera & Schneider 2007). Techniques to be used in exomoons’ detection are transit timing variations (TTVs), transit duration variations (TDVs), and apparent planetary transit radius variations (TRVs) (Rodenbeck, Heller & Gizon 2020); according to Rodenbeck, Heller & Gizon (2020), TRVs could be a more promising means to identify exomoons in large exoplanet surveys.

It is expected that an exomoon, tidally locked to its parent planet but not to the host star, moves in the planetary equatorial plane due to the Kozai mechanism and tidal evolution (Porter & Grundy 2011; Heller & Barnes 2013). Moreover, the satellite’s spin S should be parallel to the orbital angular momentum L of the planetocentric motion (Heller & Barnes 2013). Thus, the exomoon should have the same obliquity with respect to the circumstellar orbit as the planetary

¹See, e.g., <http://phl.upr.edu/projects/habitable-exoplanets-catalog> and <http://exoplanet.eu/> on the Internet.

spin \mathbf{J} (Heller & Barnes 2013), so that it could experience seasons if the equator of the host planet is tilted against the ecliptic plane (Heller & Barnes 2013). It seems to be just the case for a gaseous giant since massive host planets of exomoons can maintain significant obliquities on timescales quite large (Heller, Leconte & Barnes 2011; Heller & Barnes 2013).

One of the key parameters for the long-term habitability of an astronomical major body is the value of the angle ε , usually known as obliquity, of its spin to the plane of the orbital motion about its main source of electromagnetic irradiation (Barnes et al. 2016), and its long-term stability over the æons. In the case of, say, a star-planet scenario, the planetary axial tilt² ε_\star to the ecliptic plane is crucial for the insolation received from the host star (Laskar, Joutel & Robutel 1993; Williams & Kasting 1997; Laskar et al. 2004; Armstrong et al. 2014; Linsenmeier, Pascale & Lucarini 2015; Quarles et al. 2019; Kilic, Raible & Stocker 2017; Shan & Li 2018; Quarles, Li & Lissauer 2019). Indeed, variations in obliquity $\Delta\varepsilon_\star(t)$ drive changes in planetary climate. If $\Delta\varepsilon_\star(t)$ are rapid and/or large, the resulting climate shifts can be commensurately severe, as pointed out by, e.g., Armstrong, Leovy & Quinn (2004). As far as the Earth is concerned, its obliquity changes slowly with time from $\approx 22^\circ.1$ to $24^\circ.5$, undergoing an oscillation cycle with amplitude $\lesssim 2^\circ.4$ in about 41,000 yr (Quarles, Li & Lissauer 2019). The value of the Earth’s obliquity impacts the seasonal cycles and its long-term variation affects the terrestrial climate (Milankovitch 1941), as deduced from geologic records (Kerr 1987; Mitrovica & Forte 1995; Pais et al. 1999). In the case of an exomoon³, in addition to the stellar light directly hitting it, other bolometric components of the electromagnetic input come into play because of the stellar reflected light by the planet and the planet’s own infrared irradiation Heller & Barnes (2013). Thus, it is arguable that, in addition to ε_\star , also the long-term changes of the obliquity⁴ ε_p of S to the circumplanetary orbital plane may affect the climate of the exomoon.

The purpose of this paper is to show, for the first time, that GTR may directly affects the habitability of an exomoon through the gravitoelectric de Sitter (de Sitter 1916; Schouten 1918; Fokker 1920) and gravitomagnetic Lense-Thirring⁵ (Pugh 1959; Schiff 1960) precessions of its spin \mathbf{S} induced by the post-Newtonian (pN) static de Sitter and stationary Lense-Thirring components of the gravitational field of its parent planet (Ohanian & Ruffini 2013; Poisson & Will 2014). To the benefit of a reader not acquainted with GTR, the pN expansion is one of the most successful and famous approximation schemes that have been developed in the past

²Here, the symbol \star appended to the angle ε means that the latter is referred to the plane of the planetary orbit around the host star, dubbed as ecliptic plane.

³Also tidal heating enters the total energy budget determining the habitability of an exomoon (Heller & Barnes 2013).

⁴Here, the subscript p refers to the plane of the satellite’s orbital motion around the planet.

⁵Such a denomination for the pN spin precession induced by the primary’s angular momentum has become of common use, despite it was discovered by Pugh and Schiff in the sixties of the twentieth century.

years for solving the fully nonlinear Einstein’s equations to describe motions of arbitrary shaped, massive bodies (Asada & Futamase 1997; Blanchet 2003; Will 2018). Furthermore, the terms “gravitoelectric” and “gravitomagnetic” have nothing to do with electric charges and currents, referring, instead, to the formal resemblance of the linearized Einstein field equations of GTR, valid in the slow-motion and weak-field approximation, with the linear Maxwellian equations of electromagnetism (Thorne, MacDonald & Price 1986; Mashhoon 2001; Rindler 2001). Both such effects were successfully measured some years ago in the dedicated spaceborne experiment Gravity Probe B (GP-B) with four artificial gyroscopes orbiting in the field of the Earth (Everitt et al. 2011, 2015). The de Sitter precession was detected also by monitoring the heliocentric motion of the Earth-Moon system (Williams, Newhall & Dickey 1996; Williams & Folkner 2009; Hofmann & Müller 2018), thought of as a giant natural gyroscope, with the Lunar Laser Ranging (LLR) technique (Dickey et al. 1994), and in some binary pulsar systems as well (Breton et al. 2008; Kramer 2012).

For the sake of definiteness, I will adopt the scenario by Heller & Barnes (2013) consisting of a main sequence star orbited at 1 astronomical unit (au) by a gravitationally bound restricted two-body system made of a Jupiter-like planet and a telluric exomoon which, under not too restrictive assumptions, may harbour life. In fact, exomoons may exist also in the habitable zone of M dwarfs (Martínez-Rodríguez et al. 2019; Trifonov et al. 2020), but, in this case, the analysis would be more involved because of the direct dynamical effects of the star itself. It will be shown that, for the range of plausible distances allowed to the exomoon in order to be habitable (Heller & Barnes 2013), the obliquity ε_\star of S to the ecliptic plane may undergo huge variations of tens of degrees over $\simeq 0.1 - 1$ Myr. More specifically, I will neglect the presence of other planets in the system, so that the ecliptic plane, assumed as reference coordinate $\{x, y\}$ plane, stay fixed. The orbit of the exomoon around its host planet will be assumed to be circular, with a size of, say, 5 to 10 planetary radii R (Heller & Barnes 2013). As far as the exomoon’s primary is concerned, I will, first, assume the physical parameters of Jupiter for it. Then, I will look also at another more massive, larger and more rapidly spinning prototypical gaseous giant planet having the properties of one of those recently characterized in Bryan et al. (2020). All the three tilting angles⁶ η_\star , $I_\star \varepsilon_\star$ to the ecliptic of J , L , S will be taken equal to the Earth’s obliquity, i.e. $23^\circ 44'$; actually, similar scenario exists in our Solar System, being represented by Saturn and Titan whose spins are tilted by $\simeq 26^\circ 7'$ to the ecliptic. Nonetheless, I will allow for more or less marked departures from the ideal alignment condition by varying, say, their azimuthal angles and, in another set of runs, by introducing small offsets in both their spherical angles for all the three angular momenta; if they were perfectly parallel, no pN spin precessions would occur at all, as it will be shown in Section 2. It should be stressed that, by placing the planet-satellite system at 1 au from the star, the GTR spin precessions considered here are not due to the pN components of the star’s gravitational field; moreover, it can be reasonably assumed that the ecliptic plane is not perturbed too much by the

⁶In the following, I will omit the subscript \star from them; the variations of ε_p will not be considered.

post-Keplerian (pK), Newtonian or pN, components of the stellar field which are able to induce long-term orbital variations. Instead, they are induced by the planet’s pN field itself; thus, the sources of the de Sitter and Lense-Thirring precessions of the exomoon’s spin are the mass M and the spin angular momentum \mathbf{J} of the Jupiter-type gas giant, respectively (Ohanian & Ruffini 2013; Poisson & Will 2014). As such, they are present independently of any peculiar characteristic of the exomoon itself like, e.g., its quadrupole mass moment, tidal Love number, etc., which may induce their own long-term changes in the obliquity of its spin.

The paper is organized as follows. In Section 2, analytical expressions for the pN rates of change of the satellite’s spin axis with respect to a fixed reference plane are derived. They are numerically integrated for the case of a Jupiter-like host planet in Section 3, and for a different gaseous giant body in Section 4 by suitably varying the system’s parameter space in both cases. Section 5 summarizes my findings and offer my conclusions.

2. The de Sitter and Lense-Thirring precessions of the spin’s obliquity to the ecliptic plane

Let me assume a coordinate system whose reference $\{x, y\}$ plane coincides with the ecliptic plane of the planet-satellite binary. As parameterization of the satellite’s spin axis $\hat{\mathbf{S}}$, I adopt

$$\hat{S}_x = \sin \varepsilon \cos \alpha, \quad (1)$$

$$\hat{S}_y = \sin \varepsilon \sin \alpha, \quad (2)$$

$$\hat{S}_z = \cos \varepsilon, \quad (3)$$

so that α is the spin’s azimuthal angle and ε is its obliquity to the ecliptic: $\varepsilon = 0^\circ$ means that the spin is perpendicular to it. From Equations (1)-(3), it can be straightforwardly obtained

$$\frac{d\varepsilon}{dt} = -\csc \varepsilon \frac{d\hat{S}_z}{dt}, \quad (4)$$

$$\frac{d\alpha}{dt} = \csc \varepsilon \left(\cos \alpha \frac{d\hat{S}_y}{dt} - \sin \alpha \frac{d\hat{S}_x}{dt} \right). \quad (5)$$

To the pN order, the general relativistic rates of change of ε , α , averaged over one orbital revolution of the satellite about its parent planet, can be inferred from the sum of the pN de Sitter and Lense-Thirring averaged precessions of $\hat{\mathbf{S}}$

$$\frac{d\hat{\mathbf{S}}}{dt} = (\boldsymbol{\Omega}_{\text{ds}} + \boldsymbol{\Omega}_{\text{LT}}) \times \hat{\mathbf{S}}, \quad (6)$$

where (Barker & O’Connell 1975; Poisson & Will 2014)

$$\mathbf{\Omega}_{\text{dS}} = \frac{3 n_{\text{b}} \mu}{2 c^2 a (1 - e^2)} \hat{\mathbf{L}}, \quad (7)$$

$$\mathbf{\Omega}_{\text{LT}} = \frac{G J}{2 c^2 a^3 (1 - e^2)^{3/2}} \left[\hat{\mathbf{J}} - 3 (\hat{\mathbf{J}} \cdot \hat{\mathbf{L}}) \hat{\mathbf{L}} \right]. \quad (8)$$

In Equations (7)-(8), c is the speed of light in vacuum, G is the Newtonian gravitational constant, $\mu \doteq GM$ is the planet’s gravitational parameter, a , e are the semimajor axis and the eccentricity, respectively, of the satellite’s planetocentric orbit, $n_{\text{b}} = \sqrt{\mu/a^3}$ is the Keplerian mean motion, $\hat{\mathbf{L}} = \{\sin I \sin \Omega, -\sin I \cos \Omega, \cos I\}$ is the unit vector of the orbital angular momentum. By parameterizing the planet’s spin axis $\hat{\mathbf{J}}$ as

$$\hat{J}_x = \sin \eta \cos \varphi, \quad (9)$$

$$\hat{J}_y = \sin \eta \sin \varphi, \quad (10)$$

$$\hat{J}_z = \cos \eta, \quad (11)$$

from Equations (1)-(11), one finally gets

$$\begin{aligned} \frac{d\varepsilon}{dt} = & -\frac{3 n_{\text{b}} \mu \sin I \cos \zeta}{2 c^2 a (1 - e^2)} + \\ & + \frac{G J}{4 c^2 a^3 (1 - e^2)^{3/2}} \left[\sin \eta (\sin \xi - 3 \sin \chi) + 3 \cos \zeta (\cos \eta \sin 2I + 2 \cos^2 I \sin \eta \sin \psi) \right], \end{aligned} \quad (12)$$

$$\begin{aligned} \frac{d\alpha}{dt} = & \frac{3 n_{\text{b}} \mu (\cos I + \cot \varepsilon \sin I \sin \zeta)}{2 c^2 a (1 - e^2)} - \\ & - \frac{G J}{8 c^2 a^3 (1 - e^2)^{3/2}} \left\{ \cos \eta (2 + 6 \cos^2 I - 6 \sin^2 I + 6 \cot \varepsilon \sin 2I \sin \zeta) + \right. \\ & \left. + \sin \eta [(\cos \xi + 3 \cos \chi) \cot \varepsilon - 6 (\sin 2I - \cos 2I \cot \varepsilon \sin \zeta) \sin \psi] \right\}, \end{aligned} \quad (13)$$

with

$$\zeta \doteq \alpha - \Omega, \quad (14)$$

$$\xi \doteq \alpha - \varphi, \quad (15)$$

$$\psi \doteq \varphi - \Omega, \quad (16)$$

$$\chi \doteq \varphi + \alpha - 2\Omega. \quad (17)$$

In terms of the parameterization of Equations (1)-(3) and Equations (9)-(11), the azimuthal angle Ξ of $\hat{\mathbf{L}}$ is related to the longitude of the ascending node Ω by

$$\Omega = 90^\circ + \Xi. \quad (18)$$

If $\hat{\mathbf{S}}$, $\hat{\mathbf{L}}$, $\hat{\mathbf{J}}$ are aligned, i.e. for $\varepsilon = I = \eta$, $\alpha = \Xi = \varphi$, it is

$$\zeta = -90^\circ, \quad (19)$$

$$\xi = 0, \quad (20)$$

$$\psi = -90^\circ, \quad (21)$$

$$\chi = -180^\circ, \quad (22)$$

so that Equations (12)-(13) vanish.

In obtaining the averaged rates of Equations (12)-(13), it was assumed that ε , α stay essentially constant over one satellite's orbital period, and that I , Ω are fixed, i.e. a Keplerian ellipse was used as unperturbed, reference trajectory in the averaging procedure. In fact, a long-term modulation is introduced in Equations (12)-(13) by I , Ω since, actually, they do vary because of a number of classical and general relativistic pK precessions the most important of which are the classical ones due to the planetary oblateness J_2 and the pN Lense-Thirring effect caused by the planet's spin \mathbf{J} . By using Equations (1)-(3) and Equations (9)-(11), the classical and relativistic pK averaged rates of change of I , Ω for an arbitrary orientation of the primary's spin axis (Barker & O'Connell 1975; Damour & Schafer 1988; Damour & Taylor 1992; Will 2008;

Iorio 2017)

$$\frac{dI}{dt} = -\frac{3 n_b R^2 J_2 (\hat{\mathbf{J}} \cdot \hat{\mathbf{l}}) (\hat{\mathbf{J}} \cdot \hat{\mathbf{h}})}{2 a^2 (1 - e^2)^2} + \frac{2 G J (\hat{\mathbf{J}} \cdot \hat{\mathbf{l}})}{c^2 a^3 (1 - e^2)^{3/2}}, \quad (23)$$

$$\frac{d\Omega}{dt} = -\frac{3 n_b R^2 J_2 \csc I (\hat{\mathbf{J}} \cdot \hat{\mathbf{m}}) (\hat{\mathbf{J}} \cdot \hat{\mathbf{h}})}{2 a^2 (1 - e^2)^2} + \frac{2 G J \csc I (\hat{\mathbf{J}} \cdot \hat{\mathbf{m}})}{c^2 a^3 (1 - e^2)^{3/2}} \quad (24)$$

can be cast into the form

$$\begin{aligned} \frac{dI}{dt} = & \frac{3 n_b R^2 J_2 \cos \psi \sin \eta (-\cos I \cos \eta + \sin I \sin \eta \sin \psi)}{2 a^2 (1 - e^2)^2} + \\ & + \frac{2 G J \sin \eta \cos \psi}{c^2 a^3 (1 - e^2)^{3/2}}, \end{aligned} \quad (25)$$

$$\begin{aligned} \frac{d\Omega}{dt} = & -\frac{3 n_b R^2 J_2 \sin I (\cos \eta + \cot I \sin \eta \sin \psi) (\cot I \cos \eta - \sin \eta \sin \psi)}{2 a^2 (1 - e^2)^2} + \\ & + \frac{2 G J (\cos \eta + \cot I \sin \eta \sin \psi)}{c^2 a^3 (1 - e^2)^{3/2}}. \end{aligned} \quad (26)$$

Equations (23)-(24) can be expressed in compact, vectorial form as (Barker & O’Connell 1975)

$$\frac{d\hat{\mathbf{L}}}{dt} = (2 \boldsymbol{\Omega}_{\text{dS}} + 4 \boldsymbol{\Omega}_{\text{LT}} + \boldsymbol{\Omega}_{J_2}) \times \hat{\mathbf{L}}, \quad (27)$$

where $\boldsymbol{\Omega}_{\text{dS}}$, $\boldsymbol{\Omega}_{\text{LT}}$ are given by Equations (7)-(8), respectively, and (Barker & O’Connell 1975)

$$\boldsymbol{\Omega}_{J_2} = -\frac{3 n_b J_2 R^2}{4 a^2 (1 - e^2)^2} \left\{ 2 (\hat{\mathbf{J}} \cdot \hat{\mathbf{L}}) \hat{\mathbf{J}} + \left[1 - 5 (\hat{\mathbf{J}} \cdot \hat{\mathbf{L}})^2 \right] \hat{\mathbf{L}} \right\}. \quad (28)$$

Equations (25)-(26) vanish for Equations (19)-(22). Thus, also the orbital angular momentum stay fixed in space if $\hat{\mathbf{S}}$, $\hat{\mathbf{L}}$, $\hat{\mathbf{J}}$ are aligned, as it can straightforwardly be inferred from Equations (7)-(8) and Equation (27).

Equations (12)-(13) and Equations (25)-(26) represent a system of nonlinear first order differential equations for the four unknowns⁷ $\varepsilon(t)$, $\alpha(t)$, $I(t)$, $\Omega(t)$ to be simultaneously integrated.

⁷The angles η , φ of $\hat{\mathbf{J}}$ are assumed to be constant.

3. The case of a Jupiter-like parent planet

I numerically did it over 1 Myr for a fictitious exomoon circling, first, a planet with the same physical parameters of Jupiter along a circular orbit at a few radii from it, as per Heller & Barnes (2013). I did not assume an exact alignment of \mathbf{S} , \mathbf{L} , \mathbf{J} by allowing for different values of, say, their azimuthal angles α_0 , Ω_0 , φ . Thus, I adopted the initial conditions $\varepsilon_0 = I_0 = \eta = 23^\circ.44$, $\varphi = 60^\circ$, $\alpha_0 = 150^\circ$, $\Omega_0 = 50^\circ$, $a = 5 R$, $e = 0$ by varying each of them in several runs with the exception of η , I_0 , ε_0 which were held fixed to $23^\circ.44$ in all of them. In particular, I stress my choice for ε_0 in order to have a scenario as close as possible to that of the Sun-Earth system in regard to the stellar insolation. A similar case is, in fact, present in our Solar System, apart from the system’s distance from the Sun: Saturn⁸, whose spin’s obliquity to the ecliptic is (Ward & Hamilton 2004) $\eta = 26^\circ.7$, and its moon Titan, at $20 R$ from it, whose spin angular momentum \mathbf{S} is tilted by just (Stiles et al. 2008) $\simeq 0.3^\circ$ to its orbital plane which, in turn, lies in the equator of Saturn up to an offset as little as 0.33° (Murray & Dermott 2000, Table A.9). In Figure 1, I show the resulting time series for the pN shift $\Delta\varepsilon(t)$ of the satellite’s spin obliquity to the plane of the binary’s orbit about the parent star.

⁸In the case of the Saturn-Titan system, by using the HORIZONS web interface, maintained by the NASA Jet propulsion Laboratory (JPL), for the inclination and the node at epoch of the Kronocentric orbit of Titan referred to the International Celestial Reference Frame (ICRF), and Seidelmann et al. (2007) for the right ascension (RA) and declination (DEC) at the same epoch of the spin axes of Saturn and Titan, it is possible to infer that the angles ϑ between \mathbf{S} , \mathbf{L} , \mathbf{J} are as little as $\vartheta_{SJ} \simeq 0.6^\circ$, $\vartheta_{SL} \simeq 0.3^\circ$, $\vartheta_{JL} \simeq 0.4^\circ$.

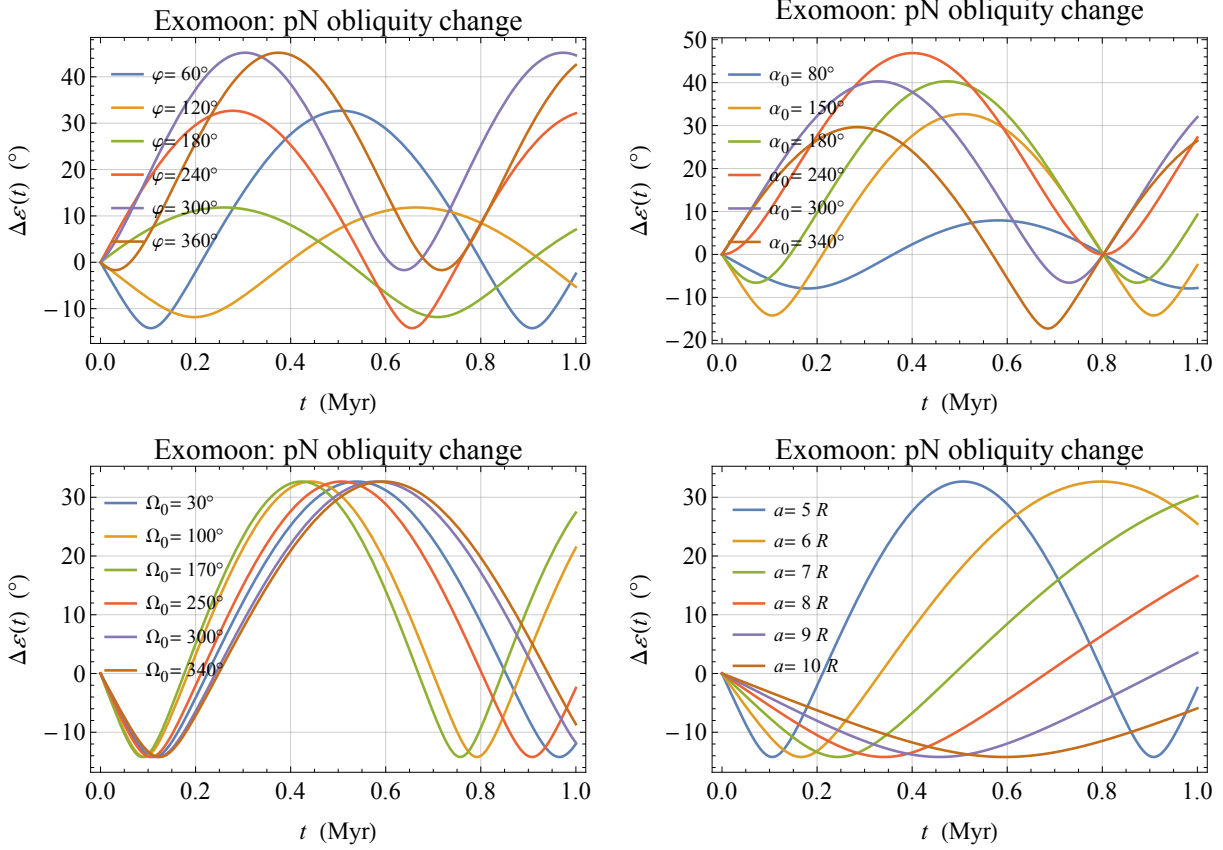


Fig. 1.— Numerically produced time series $\Delta\epsilon(t)$, in $^\circ$, of the general relativistic pN variation of the obliquity ϵ to the ecliptic plane of the spin axis $\hat{\mathbf{S}}$ of a putative exomoon orbiting a gaseous giant planet with the same physical properties of Jupiter. They were obtained by simultaneously integrating the orbit-averaged Equations (12)-(13) and Equations (25)-(26) for the rates of change of $\epsilon(t)$, $\alpha(t)$, $\Omega(t)$, $I(t)$ over 1 Myr. Here, $\epsilon(t)$, $\alpha(t)$ are the polar angles of $\hat{\mathbf{S}}$ according to the parameterization $\hat{S}_x = \sin \epsilon \cos \alpha$, $\hat{S}_y = \sin \epsilon \sin \alpha$, $\hat{S}_z = \cos \epsilon$, while $\Omega(t)$, $I(t)$ are the longitude of the ascending node and the inclination, respectively, of the satellite’s planetocentric orbit which undergoes long-term variations mainly due to the planetary quadrupole mass moment J_2 . The parameterization adopted for the planet’s spin axis $\hat{\mathbf{J}}$ is $\hat{J}_x = \sin \eta \cos \varphi$, $\hat{J}_y = \sin \eta \sin \varphi$, $\hat{J}_z = \cos \eta$, with η , φ kept fixed. The initial conditions common to all the panels are $I_0 = \eta = \epsilon_0 = 23^\circ.44$, where I_0 and ϵ_0 are the initial values of the inclination of the orbital plane and of the obliquity of the satellite’s spin axis, respectively. In the upper left panel, the values $a = 5 R$, $\Omega_0 = 50^\circ$, $\alpha_0 = 150^\circ$ were adopted (a is the semimajor axis of the satellite’s planetocentric orbit, while Ω_0 , α_0 are the initial values of the longitude of the ascending node and of the azimuthal angle of $\hat{\mathbf{S}}$, respectively), while in the other ones, $\varphi = 60^\circ$ was used, all other things being equal.

It can be seen that it experiences substantial variations over timescales of 1 Myr whose amplitudes can be as large as few tens of degrees up to $\approx 40 - 70^\circ$. Importantly, such a feature

is not limited just to some particular set of initial conditions, being, instead, common to a wide range of them.

I checked the validity of Figure 1, based on the orbit-averaged Equations (12)-(13) and Equations (25)-(26), by simultaneously integrating, in standard pN isotropic coordinates, the fully general relativistic equations for both the parallel transport of the spin 4-vector \mathbf{S} of a pointlike gyroscope freely moving in the stationary spacetime of a localized mass-energy source endowed with mass monopole (M) and quadrupole (J_2), and spin dipole (\mathbf{J}) moments, and the four dimensional gyro's geodesic equations for its orbital motion as well over 0.001 Myr. I adopted the same orbital and physical parameters of the previous integration along with the same initial conditions. Then, I computed the time series for $\varepsilon(t)$ from the solution for $\hat{S}_z(t)$, which is one of the eight unknowns represented by the components of the gyro's spin and position 4-vectors, as $\varepsilon(t) = \arccos \hat{S}_z(t)$. I found an agreement with the outcome of Figure 1 to within $\simeq 10^{-5}^\circ$.

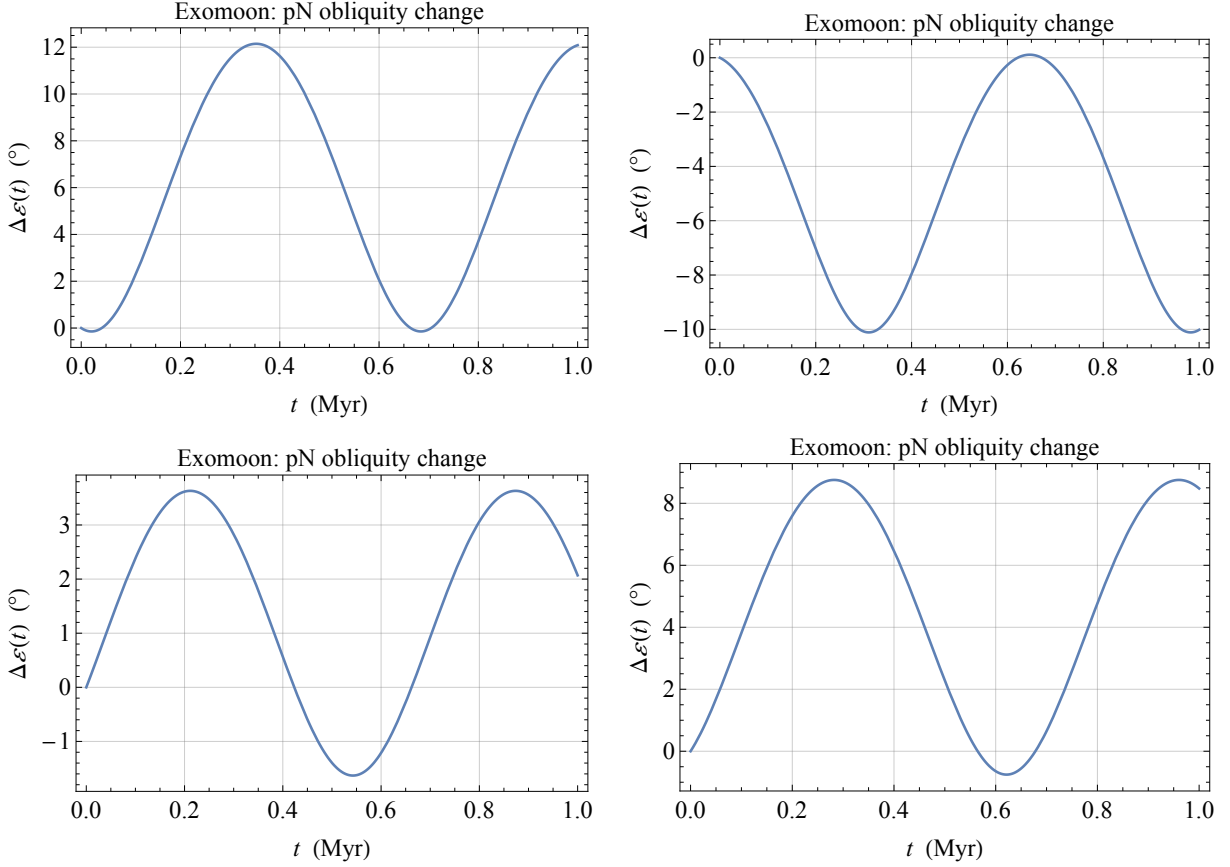


Fig. 2.— Numerically produced time series $\Delta\varepsilon(t)$, in $^\circ$, of the general relativistic pN variation of the obliquity ε to the ecliptic plane of the spin axis \hat{S} of a putative exomoon orbiting a gaseous giant planet with the same physical properties of Jupiter. They were obtained by simultaneously integrating the orbit-averaged Equations (12)-(13) and Equations (25)-(26) for the rates of change of $\varepsilon(t)$, $\alpha(t)$, $\Omega(t)$, $I(t)$ over 1 Myr. Here, $\varepsilon(t)$, $\alpha(t)$ are the polar angles of \hat{S} according to the parameterization $\hat{S}_x = \sin \varepsilon \cos \alpha$, $\hat{S}_y = \sin \varepsilon \sin \alpha$, $\hat{S}_z = \cos \varepsilon$, while $\Omega(t)$, $I(t)$ are the longitude of the ascending node and the inclination, respectively, of the satellite’s planetocentric orbit which undergoes long-term variations mainly due to the planetary quadrupole mass moment J_2 . The parameterization adopted for the planet’s spin axis \hat{J} is $\hat{J}_x = \sin \eta \cos \varphi$, $\hat{J}_y = \sin \eta \sin \varphi$, $\hat{J}_z = \cos \eta$, with η , φ kept fixed. The initial conditions common to all the panels are $a = 5 R$, $e = 0$, $\varepsilon_0 = 23^\circ.44$, $\alpha_0 = 150^\circ$, while in each panel I_0 , η , Ω_0 , φ were varied with respect to ε_0 , α_0 by small offsets δ_x , $x = I, \eta, \Omega, \varphi$ according to $I_0 = \varepsilon_0 + \delta_I$, $\eta = \varepsilon_0 + \delta_\eta$, $\Omega_0 = 90^\circ + \alpha_0 + \delta_\Omega$, $\varphi = \alpha_0 + \delta_\varphi$. In the upper left panel, $\delta_I = +2^\circ$, $\delta_\eta = +6^\circ$, $\delta_\Omega = -7^\circ$, $\delta_\varphi = -3^\circ$, in the upper right panel, $\delta_I = +5^\circ$, $\delta_\eta = -5^\circ$, $\delta_\Omega = +3^\circ$, $\delta_\varphi = -3^\circ$, in the lower left panel, $\delta_I = -1^\circ$, $\delta_\eta = +1^\circ$, $\delta_\Omega = +8^\circ$, $\delta_\varphi = -2^\circ$, and in the lower right panel, $\delta_I = -9^\circ$, $\delta_\eta = +4^\circ$, $\delta_\Omega = +2^\circ$, $\delta_\varphi = +6^\circ$.

In producing Figure 2, I assumed a close, although not perfect, alignment of \hat{S} , \hat{L} , \hat{J} allowing for small offsets of just a few degrees with respect to the values $23^\circ.44$ for the obliquity and

150° for the azimuthal angle, all the rest being equal as in Figure 1. The resulting shifts $\Delta\epsilon(t)$ are still potentially significant for life since their amplitudes are of the order of $\simeq 5^\circ - 12^\circ$ over characteristic timescales as short as $\simeq 0.6$ Myr.

The obliquity of the exomoon’s spin axis to the system’s ecliptic plane can, in principle, vary also because of torques of classical origin which, however, depend on the peculiar characteristics of the satellite like, e.g., its tidal response. Instead, the pN effects previously investigated are due only to the spacetime itself deformed by the mass-energy currents of the parent planet.

Variations of the insolation received by the exomoon from the host star due to changes in ϵ so large as those exhibited by Figure 1, which would affect also the amount of radiation received by the planet as well, can certainly have a sensible impact on its habitability, representing a novel element which should be taken into account in future studies on the capability of such worlds to sustain life.

4. The case of faster spinning, larger and more massive gaseous giant planets

Until now, I limited myself to the case of a host planet with the same Jovian physical parameters. It is important to look also at other possible gaseous giants with different fundamental characteristics with respect to Jupiter. Recently, for some of them orbiting at a few tens or hundreds of astronomical units from their parent stars, it was possible to determine some key parameters like the mass M , the equatorial radius R and the spinning period P (Bryan et al. 2020). In order to assess the pN effects on the spin axis of possible exomoons of similar planets, I need estimates of their dimensionless quadrupole mass moment J_2 and their spin angular momentum J .

Let me assume that the gas giant of interest can be modeled as an axisymmetric ellipsoid in hydrostatic equilibrium. By defining (Ragozzine & Wolf 2009; Leconte, Lai & Chabrier 2011)

$$q \doteq \frac{4\pi^2 R^3}{P^2 \mu}, \quad (29)$$

its first even zonal harmonic can be cast into the form (Ragozzine & Wolf 2009; Leconte, Lai & Chabrier 2011)

$$J_2 = \frac{k_2}{3} q, \quad (30)$$

where k_2 is the Love number (Sterne 1939; Kopal 1959; Ragozzine & Wolf 2009; Leconte, Lai & Chabrier 2011). By adopting the commonly used $n = 1$ polytrope to approximate the density structure of (cold) gas giant planets, it turns out that (Kopal 1959)

$$k_2 \simeq 0.52. \quad (31)$$

The planetary spin angular momentum can approximately be expressed as

$$J = j M R^2 \left(\frac{2\pi}{P} \right), \quad (32)$$

where j is the moment of inertia factor which, according to the Darwin-Radau equation, is given by (Bourda & Capitaine 2004)

$$j = \frac{2}{3} \left(1 - \frac{2}{5} \sqrt{1 + \beta} \right), \quad (33)$$

with

$$\beta = \frac{5q}{2f} - 2. \quad (34)$$

In Equation (34), f is the geometric flattening, defined as the difference between the planet's equatorial and polar radii normalized to the equatorial radius, which, in this case, is given by (Leconte, Lai & Chabrier 2011)

$$f = \left(\frac{k_2 + 1}{2} \right) q. \quad (35)$$

I can, now, use Equation (30) and Equation (32) to evaluate the quadrupole mass moment and the angular momentum of a gaseous giant planet with the same characteristics of, say, HD 106906b which, according to Table 3 of Bryan et al. (2020), has $P = 4$ hr, $M = 11 M_{\text{Jup}}$, and $R = 1.56 R_{\text{Jup}}$, where M_{Jup} , R_{Jup} are referred to Jupiter. In Figure 3, I plot J_2/J_2^{Jup} , J/J_{Jup} for a range of plausible values of k_2 (Ragozzine & Wolf 2009).

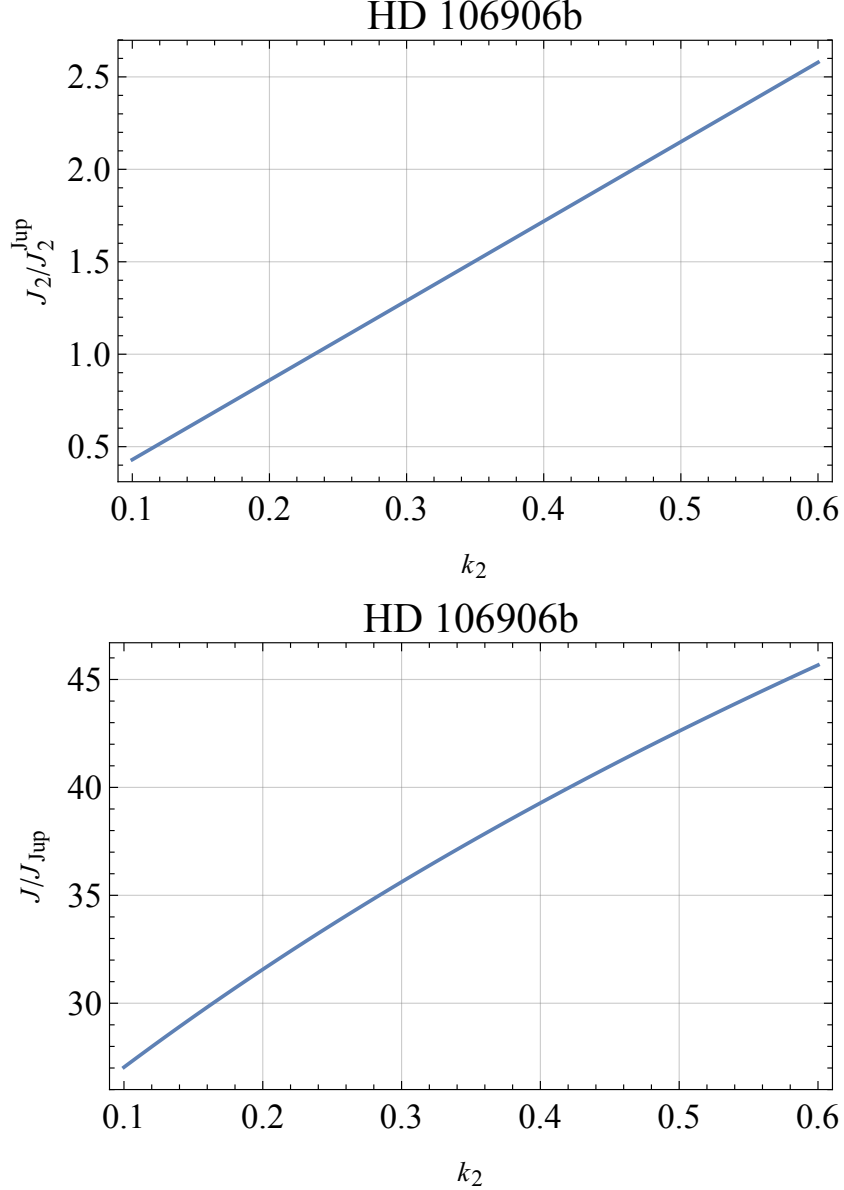


Fig. 3.— Dimensionless quadrupole mass moment J_2 and spin angular momentum J , normalized to the corresponding values for Jupiter $J_2^{\text{Jup}} = 0.0146966$ (Iess et al. 2018), $J_{\text{Jup}} = 6.9 \times 10^{38} \text{ J s}$ (Soffel et al. 2003), of the gaseous giant exoplanet HD 106906b (Bryan et al. 2020) plotted according to Equation (30) and Equation (32) as functions of the Love number k_2 within a range of plausible values for it retrieved from Ragozzine & Wolf (2009).

It can be noted from it that J , J_2 can be up to $\simeq 45$ and $\simeq 2.5$ times larger than the Jovian values.

In Figure 4, I depict the numerically integrated time series of $\Delta\epsilon(t)$ in the case of an exoplanet

with the same mass, equatorial radius and spinning period of HD109906b, and $k_2 = 0.52$.

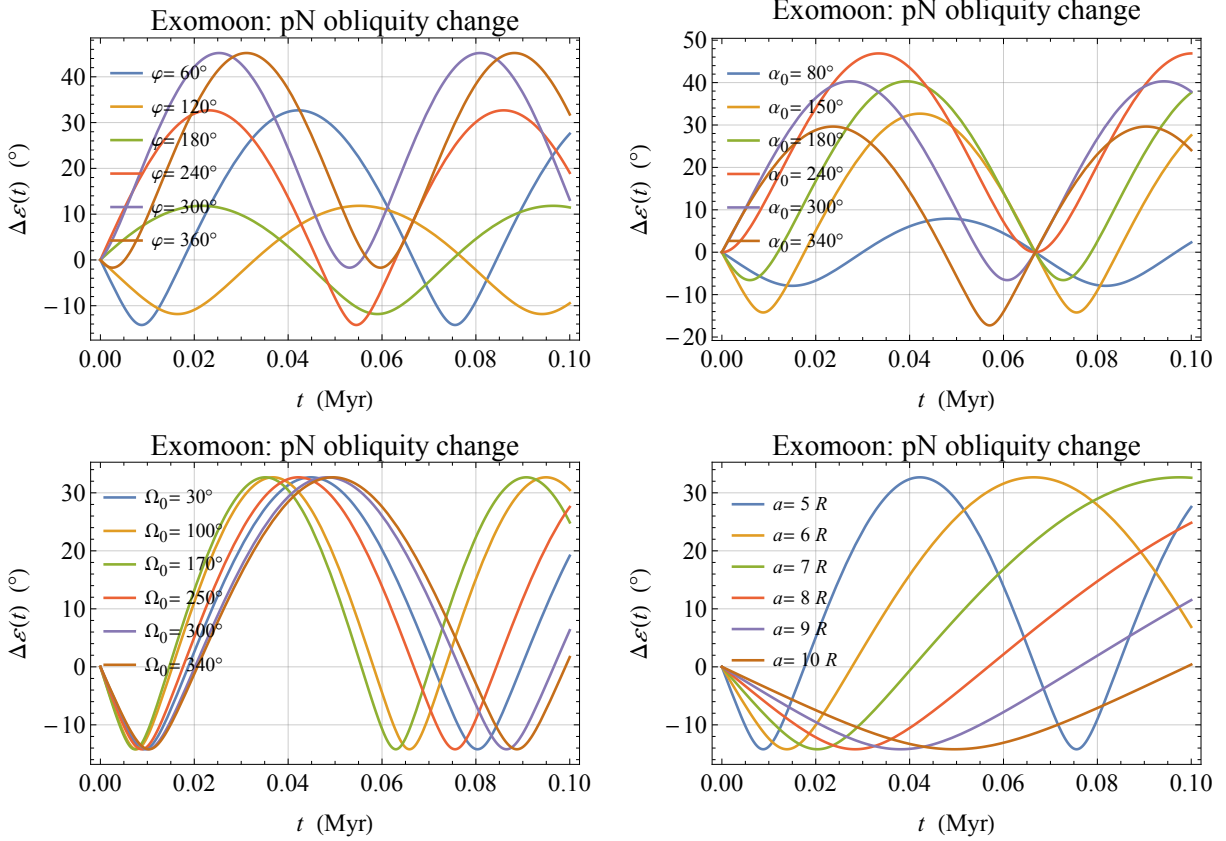


Fig. 4.— Numerically produced time series $\Delta\epsilon(t)$, in $^\circ$, of the general relativistic pN variation of the obliquity ϵ to the ecliptic plane of the spin axis \hat{S} of a putative exomoon orbiting a gaseous giant planet with the same mass, equatorial radius and spinning period of HD109906b ($P = 4$ hr, $M = 11 M_{\text{Jup}}$, $R = 1.56 R_{\text{Jup}}$) (Bryan et al. 2020), and with J_2 and J computed with Equation (30) and Equation (32) for $k_2 = 0.52$. They were obtained by simultaneously integrating the orbit-averaged Equations (12)-(13) and Equations (25)-(26) for the rates of change of $\epsilon(t)$, $\alpha(t)$, $\Omega(t)$, $I(t)$ over 0.1 Myr. Here, $\epsilon(t)$, $\alpha(t)$ are the polar angles of \hat{S} according to the parameterization $\hat{S}_x = \sin \epsilon \cos \alpha$, $\hat{S}_y = \sin \epsilon \sin \alpha$, $\hat{S}_z = \cos \epsilon$, while $\Omega(t)$, $I(t)$ are the longitude of the ascending node and the inclination, respectively, of the satellite’s planetocentric orbit which undergoes long-term variations mainly due to the planetary quadrupole mass moment J_2 . The parameterization adopted for the planet’s spin axis \hat{J} is $\hat{J}_x = \sin \eta \cos \varphi$, $\hat{J}_y = \sin \eta \sin \varphi$, $\hat{J}_z = \cos \eta$, with η , φ kept fixed. The initial conditions common to all the panels are $I_0 = \eta = \epsilon_0 = 23^\circ.44$, where I_0 and ϵ_0 are the initial values of the inclination of the orbital plane and of the obliquity of the satellite’s spin axis, respectively. In the upper left panel, the values $a = 5 R$, $\Omega_0 = 50^\circ$, $\alpha_0 = 150^\circ$ were adopted (a is the semimajor axis of the satellite’s planetocentric orbit, while Ω_0 , α_0 are the initial values of the longitude of the ascending node and of the azimuthal angle of \hat{S} , respectively), while in the other ones, $\varphi = 60^\circ$ was used, all other things being equal.

Also in this case, I kept the obliquities ε_0 , I_0 , η fixed to $23^\circ.44$ by varying their initial azimuthal angles α_0 , Ω_0 , φ . The patterns are similar to those of those in Figure 1, but the time scale is about one order of magnitude smaller amounting to $\simeq 0.1$ Myr. Figure 5, analogous to Figure 2, displays the pN shifts $\Delta\varepsilon(t)$ when $\hat{\mathbf{S}}$, $\hat{\mathbf{L}}$, $\hat{\mathbf{J}}$ are mutually aligned up to a few degrees; the adopted offsets are the same as in Figure 2. Also in this case, the size of the obliquity variations are of the order of $\simeq 3^\circ - 12^\circ$, but the characteristic timescale is $\simeq 0.06$ Myr.

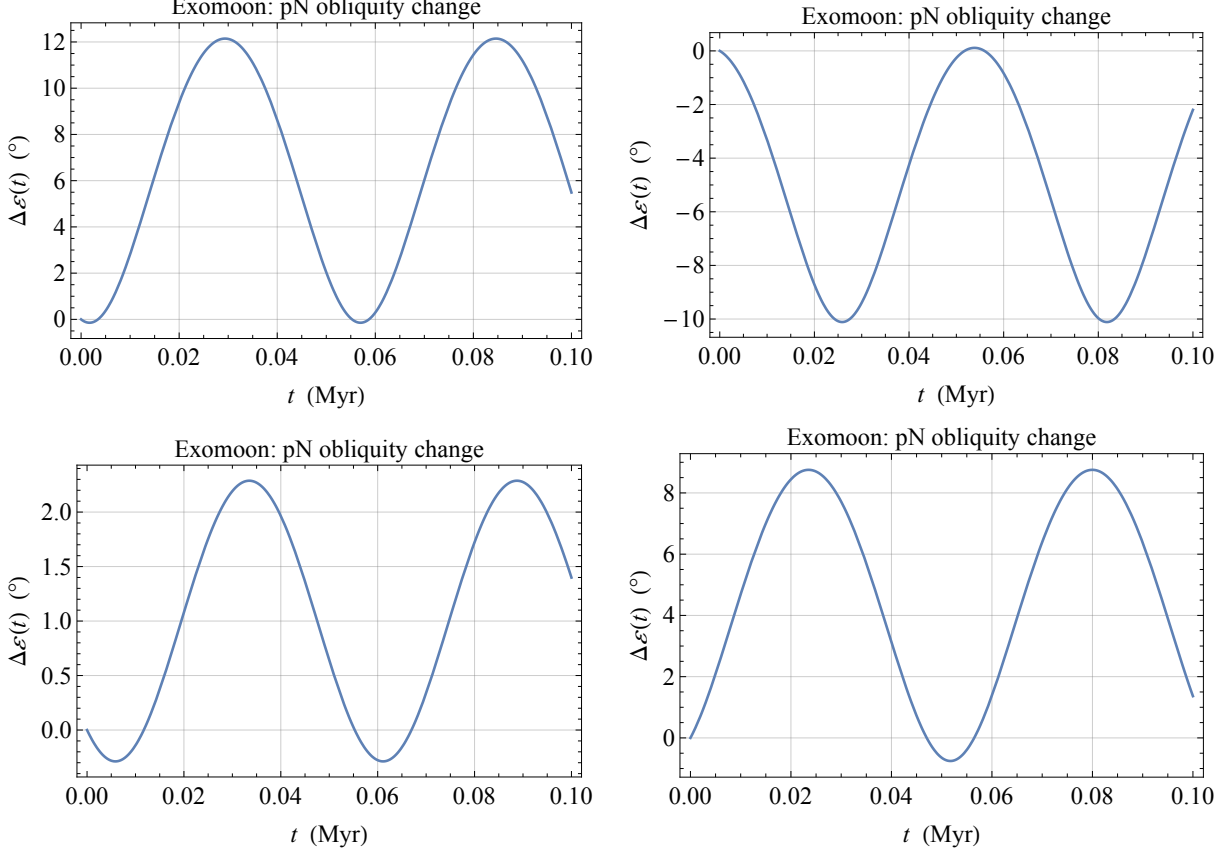


Fig. 5.— Numerically produced time series $\Delta\epsilon(t)$, in $^\circ$, of the general relativistic pN variation of the obliquity ϵ to the ecliptic plane of the spin axis \hat{S} of a putative exomoon orbiting a gaseous giant planet with the same mass, equatorial radius and spinning period of HD109906b ($P = 4$ hr, $M = 11 M_{\text{Jup}}$, $R = 1.56 R_{\text{Jup}}$) (Bryan et al. 2020), and with J_2 and J computed with Equation (30) and Equation (32) for $k_2 = 0.52$. They were obtained by simultaneously integrating the orbit-averaged Equations (12)-(13) and Equations (25)-(26) for the rates of change of $\epsilon(t)$, $\alpha(t)$, $\Omega(t)$, $I(t)$ over 1 Myr. Here, $\epsilon(t)$, $\alpha(t)$ are the polar angles of \hat{S} according to the parameterization $\hat{S}_x = \sin \epsilon \cos \alpha$, $\hat{S}_y = \sin \epsilon \sin \alpha$, $\hat{S}_z = \cos \epsilon$, while $\Omega(t)$, $I(t)$ are the longitude of the ascending node and the inclination, respectively, of the satellite’s planetocentric orbit which undergoes long-term variations mainly due to the planetary quadrupole mass moment J_2 . The parameterization adopted for the planet’s spin axis \hat{J} is $\hat{J}_x = \sin \eta \cos \varphi$, $\hat{J}_y = \sin \eta \sin \varphi$, $\hat{J}_z = \cos \eta$, with η , φ kept fixed. The initial conditions common to all the panels are $a = 5 R$, $e = 0$, $\epsilon_0 = 23.44^\circ$, $\alpha_0 = 150^\circ$, while in each panel I_0 , η , Ω_0 , φ were varied with respect to ϵ_0 , α_0 by small offsets δ_x , $x = I, \eta, \Omega, \varphi$ according to $I_0 = \epsilon_0 + \delta_I$, $\eta = \epsilon_0 + \delta_\eta$, $\Omega_0 = 90^\circ + \alpha_0 + \delta_\Omega$, $\varphi = \alpha_0 + \delta_\varphi$. In the upper left panel, $\delta_I = +2^\circ$, $\delta_\eta = +6^\circ$, $\delta_\Omega = -7^\circ$, $\delta_\varphi = -3^\circ$, in the upper right panel, $\delta_I = +5^\circ$, $\delta_\eta = -5^\circ$, $\delta_\Omega = +3^\circ$, $\delta_\varphi = -3^\circ$, in the lower left panel, $\delta_I = -1^\circ$, $\delta_\eta = +1^\circ$, $\delta_\Omega = +8^\circ$, $\delta_\varphi = -2^\circ$, and in the lower right panel, $\delta_I = -9^\circ$, $\delta_\eta = +4^\circ$, $\delta_\Omega = +2^\circ$, $\delta_\varphi = +6^\circ$.

5. Summary and Conclusions

I studied the consequences of the general relativistic post-Newtonian de Sitter and Lense-Thirring precessions of the spin of a spherically symmetric gyroscope freely moving in the deformed stationary spacetime of a massive rotating planet on the habitability of a putative exomoon orbiting a Jupiter-like gaseous giant body, assumed to be at 1 au from a Sun-type main sequence star. In particular, I looked at the long-term variations $\Delta\varepsilon(t)$ of the obliquity $\varepsilon(t)$ of the satellite's spin S to the planet-moon ecliptic plane, which is a key parameter in constraining the capability of hosting and sustaining life over long time spans since it controls the insolation received directly from the star.

I analytically derived orbit-averaged equations for the post-Newtonian rates of change of the satellite's spin obliquity $\varepsilon(t)$ and azimuthal angle $\alpha(t)$ which were numerically integrated over 1 Myr along with the equations for the precessions of the orbital inclination $I(t)$ and longitude of ascending node $\Omega(t)$ driven by both the classical quadrupole (J_2), and relativistic mass monopole (M) and spin dipole (J) components of the planetary gravitational field. I performed several runs by varying the initial conditions for the satellite's orbit around its host planet, for which the physical parameters of Jupiter were initially assumed, and the azimuthal angles of the spins of both the planet and the satellite by keeping the initial values of the spins' obliquities η , ε and of the orbital inclination I equal to the terrestrial value $23^\circ.44$ in all the integrations; the ideal condition of perfect alignment of the three angular momenta would imply the absence of any spin precessions. I successfully tested my results with another numerical integration over a trial time span 0.001 Myr long based on the fully general relativistic equations for both the parallel transport of the gyro's spin 4-vector and its four dimensional geodesic motion in the planet's spacetime. It turned out that ε undergoes huge general relativistic variations over timescales of the order of $\simeq 1$ Myr which can be as large as a few tens of degrees. Such an effect, which is independent of the satellite's own physical properties depending only on the features of the planetary deformed spacetime, is certainly of the utmost importance per se from the point of view of the capability of the exomoon of hosting and sustaining life. I considered also a configuration characterized by a closer, although not exact, alignment of the angular momenta whose orientations in space were allowed to differ by just a few degrees. Also in this case, the resulting post-Newtonian shifts of ε may be deemed as significant since they still amount to $\simeq 5^\circ - 12^\circ$ with characteristic time scales of the order of $\simeq 0.6$ Myr.

I looked also at another parent planet for which the physical parameters of the existing exoplanet HD109906b were adopted. In particular, its mass is 11 times larger than that of Jupiter, and its oblateness J_2 and spin angular momentum J can be up to 2.5 and 45 times larger than the Jovian ones. The patterns of the resulting time series and their magnitudes are similar to those for a Jupiter-like body, but its characteristic time scale is of the order of $\simeq 0.1$ Myr.

In both cases, I did not investigate the post-Newtonian variations of the obliquity of the exomoon's spin with respect to the plane of its orbit around the host planet, which may be another relevant factor in the total energy balance because of the irradiation from the planet itself due to

both the reflected sunlight and the infrared radiation. A further effect which is likely worth of further investigations is the impact of the tidal torques which, among other things, tend to align the orbital angular momentum of the planetocentric orbit with the planet and satellite's spins in order to see if they are effectively counterbalanced by the relativistic signatures obtained here.

To my knowledge, it is the first time that it is shown that general relativity may directly have a macroscopic impact on life in a likely common astronomical scenario. Future studies on the habitability of exomoons should include also such effects in the overall budget of the dynamical constraints to life sustainability.

Data availability

No new data were generated or analysed in support of this research.

REFERENCES

- Armstrong J. C., Barnes R., Domagal-Goldman S., Breiner J., Quinn T. R., Meadows V. S., 2014, *AsBio*, 14, 277
- Armstrong J. C., Leovy C. B., Quinn T., 2004, *Icar*, 171, 255
- Asada H., Futamase T., 1997, *PThPS*, 128, 123
- Barker B. M., O’Connell R. F., 1975, *PhRvD*, 12, 329
- Barnes J. W., O’Brien D. P., 2002, *ApJ*, 575, 1087
- Barnes J. W., Quarles B., Lissauer J. J., Chambers J., Hedman M. M., 2016, *AsBio*, 16, 487
- Blanchet L., 2003, in *Proceedings of the Twelfth Workshop on General relativity and Gravitation in Japan*, Shibata M., Eriguchi Y., Taniguchi K., Nakamura T., Tomita K., eds., The University of Tokyo, Komaba, Tokyo, pp. 8–23
- Bourda G., Capitaine N., 2004, *A&A*, 428, 691
- Breton R. P. et al., 2008, *Sci*, 321, 104
- Bryan M. L., Ginzburg S., Chiang E., Morley C., Bowler B. P., Xuan J. W., Knutson H. A., 2020, *ApJ*, 905, 37
- Cabrera J., Schneider J., 2007, *A&A*, 464, 1133
- Damour T., Schafer G., 1988, *NCimB*, 101, 127
- Damour T., Taylor J. H., 1992, *PhRvD*, 45, 1840
- de Sitter W., 1916, *MNRAS*, 77, 155
- Debono I., Smoot G. F., 2016, *Univ*, 2, 23
- Deeg H. J., Belmonte J. A., 2018, *Handbook of Exoplanets*. Springer, Cham
- Dickey J. O. et al., 1994, *Sci*, 265, 482
- Dobos V., Heller R., Turner E. L., 2017, *A&A*, 601, A91
- Domingos R. C., Winter O. C., Yokoyama T., 2006, *MNRAS*, 373, 1227
- Everitt C. W. F. et al., 2011, *PhRvL*, 106, 221101
- Everitt C. W. F. et al., 2015, *CQGra*, 32, 224001
- Fokker A. D., 1920, *KNAB*, 29, 611

- Forgan D., Kipping D., 2013, MNRAS, 432, 2994
- Forgan, D., 2019, IJA, 18, 510
- Fox C., Wiegert P., 2021, MNRAS, 501, 2378
- Heller R., Barnes R., 2013, AsBio, 13, 18
- Heller R., Leconte J., Barnes R., 2011, A&A, 528, A27
- Heller R. et al., 2014, AsBio, 14, 798
- Heller, R., 2012, A&A, 545, L8
- Hill M. L., Kane S. R., Seperuelo Duarte E., Kopparapu R. K., Gelino D. M., Wittenmyer R. A., 2018, ApJ, 860, 67
- Hinkel N. R., Kane S. R., 2013, ApJ, 774, 27
- Hofmann F., Müller J., 2018, CQGra, 35, 035015
- Iess L. et al., 2018, Natur, 555, 220
- Iorio L., 2017, EPJC, 77, 439
- Irwin L. N., Schulze-Makuch D., 2020, Univ, 6, 130
- Kaltenegger L., 2010, ApJ, 712, L125
- Kaltenegger L., 2017, ARA&A, 55, 433
- Kerr R. A., 1987, Sci, 235, 973
- Kilic C., Raible C. C., Stocker T. F., 2017, ApJ, 844, 147
- Kipping D. M., 2009a, MNRAS, 392, 181
- Kipping D. M., 2009b, MNRAS, 396, 1797
- Kipping D. M., Bakos G. Á., Buchhave L., Nesvorný D., Schmitt A., 2012, ApJ, 750, 115
- Kipping D. M., Forgan D., Hartman J., Nesvorný D., Bakos G. Á., Schmitt A., Buchhave L., 2013a, ApJ, 777, 134
- Kipping D. M., Fossey S. J., Campanella G., 2009, MNRAS, 400, 398
- Kipping D. M., Hartman J., Buchhave L. A., Schmitt A. R., Bakos G. Á., Nesvorný D., 2013b, ApJ, 770, 101

- Kopal Z., 1959, Close binary systems. Chapman & Hall, London
- Kramer M., 2012, in The Twelfth Marcel Grossmann Meeting. Proceedings of the MG12 Meeting on General Relativity, Damour T., Jantzen R., Ruffini R., eds., World Scientific, Singapore, pp. 241–260
- Laskar J., Joutel F., Robutel P., 1993, *Natur*, 361, 615
- Laskar J., Robutel P., Joutel F., et al., 2004, *A&A*, 428, 261
- Leconte J., Lai D., Chabrier G., 2011, *A&A*, 528, A41
- Lingam M., Loeb A., 2020, *IJA*, 19, 210
- Linsenmeier M., Pascale S., Lucarini V., 2015, *P&SS*, 105, 43
- Lissauer J. J., 2012, *NewAR*, 56, 1
- Martínez-Rodríguez H., Caballero J. A., Cifuentes C., Piro A. L., Barnes R., 2019, *ApJ*, 887, 261
- Mashhoon B., 2001, in Reference Frames and Gravitomagnetism, Pascual-Sánchez J. F., Floría L., San Miguel A., Vicente F., eds., World Scientific, Singapore, pp. 121–132
- Milankovitch M., 1941, *Kanon der Erdbestrahlung und seine Anwendung auf das Eiszeitenproblem*. Belgrad Königliche Serbische Akademie
- Misner C. W., Thorne K. S., Wheeler J. A., 2017, *Gravitation*. Princeton University Press, Princeton
- Mitrovica J. X., Forte A. M., 1995, *GeoJI*, 121, 21
- Murray C. D., Dermott S. F., 2000, *Solar System Dynamics*. Cambridge: Cambridge Univ. Press
- Ohanian H., Ruffini R., 2013, *Gravitation and Spacetime*. Third Edition. Cambridge University Press, Cambridge
- Pais M. A., Le Mouél J. L., Lambeck K., Poirier J. P., 1999, *E&PSL*, 174, 155
- Perryman M., 2018, *The Exoplanet Handbook*. Second edition. Cambridge Univ. Press, Cambridge
- Poisson E., Will C. M., 2014, *Gravity*. Cambridge: Cambridge Univ. Press
- Porter S. B., Grundy W. M., 2011, *ApJ*, 736, L14
- Pugh G., 1959, Proposal for a Satellite Test of the Coriolis Prediction of General Relativity. Research Memorandum 11, Weapons Systems Evaluation Group, The Pentagon, Washington D.C.

- Quarles B., Barnes J. W., Lissauer J. J., Chambers J., 2019, *AsBio*, 20, 73
- Quarles B., Li G., Lissauer J. J., 2019, *ApJ*, 886, 56
- Ragozzine D., Wolf A. S., 2009, *ApJ*, 698, 1778
- Rindler W., 2001, *Relativity: special, general, and cosmological*. Oxford University Press, Oxford, UK
- Rodenbeck K., Heller R., Gizon L., 2020, *A&A*, 638, A43
- Sartoretti P., Schneider J., 1999, *A&AS*, 134, 553
- Sasaki T., Stewart G. R., Ida S., 2010, *ApJ*, 714, 1052
- Schiff L., 1960, *PhRvL*, 4, 215
- Schneider J., Lainey V., Cabrera J., 2015, *IJAsB*, 14, 191
- Schouten W. J. A., 1918, *KNAB*, 27, 214
- Schulze-Makuch D., Bains W., 2018, *NatAs*, 2, 432
- Schwieterman E. W. et al., 2018, *AsBio*, 18, 663
- Seager S., 2011, *Exoplanets*. University of Arizona Press, Tucson
- Seidelmann P. K. et al., 2007, *Celestial Mechanics and Dynamical Astronomy*, 98, 155
- Shan Y., Li G., 2018, *AJ*, 155, 237
- Soffel M. et al., 2003, *AJ*, 126, 2687
- Sterne T. E., 1939, *MNRAS*, 99, 451
- Stiles B. W. et al., 2008, *AJ*, 135, 1669
- Teachey A., Kipping D. M., 2018, *SciA*, 4, eaav1784
- Teachey A., Kipping D. M., Schmitt A. R., 2018, *AJ*, 155, 36
- Thorne K. S., MacDonald D. A., Price R. H., eds., 1986, *Black Holes: The Membrane Paradigm*. Yale University Press, Yale
- Tjoa J. N. K. Y., Mueller M., van der Tak F. F. S., 2020, *A&A*, 636, A50
- Trifonov T. et al., 2020, *A&A*, 638, A16
- Ward W. R., Hamilton D. P., 2004, *AJ*, 128, 2501

Will C. M., 2008, *ApJL*, 674, L25

Will C. M., 2018, *Theory and Experiment in Gravitational Physics*. Second edition. Cambridge University Press, Cambridge

Williams D. M., Kasting J. F., 1997, *Icar*, 129, 254

Williams D. M., Kasting J. F., Wade R. A., 1997, *Natur*, 385, 234

Williams J. G., Folkner W. M., 2009, in *IAU Symposium #261*, American Astronomical Society, Vol. 261, p. 882

Williams J. G., Newhall X. X., Dickey J. O., 1996, *PhRvD*, 53, 6730

Zollinger R. R., Armstrong J. C., Heller R., 2017, *MNRAS*, 472, 8